A Regulable Internal Cavity Inside A Resorcinarene-Based Hemi-Carcerand

Kentaro Harada,† Ryo Sekiya,† and Takeharu Haino*

Abstract: Covalent organic capsules, such as carcerands and hemi-carcerands, constitute an interesting class of molecular hosts. These container molecules have confined spaces capable of hosting small molecules, although the size of the inner cavities cannot be changed substantially, limiting the scope of the applications. The title covalently linked container is produced by metal-directed dimerization of a resorcinarene-based cavitand possessing four 2,2'-bipyridyl arms on the wide rim followed by olefin metathesis at the vertexes of the resulting capsule with a second-generation Grubbs catalyst. The covalently linked bipyridyl arms permit expansion of the inner cavity by demetalation. This structural change influences the molecular recognition properties; the metal-coordinated capsule recognizes only 4,4'-diacetoxybiphenyl, while a metal-free counterpart can encapsulate not only 4,4'-diacetoxybiphenyl but also 2,5-disubstituted-1,4-bis(4-acetoxyphenylethynyl)benzene, which is 9.4 Å longer than the former guest. Molecular mechanics calculations predict that the capsule expands the internal cavity to encapsulate the long guest by unfolding the folded conformation of the alkyl chains, demonstrating the flexible and regulable nature of the cavity. The guest competition experiments show that the preferred guest can be switched by metalation and demetalation. This external stimuli-responsible guest exchange can be utilized for the development of functional supramolecular systems controlling the uptake, transport and release of chemicals.

Introduction

Molecular recognition is a key function of supramolecular chemistry. The internal space provided by hosts enables encapsulation of small to medium-sized molecules, permitting their applications for the encapsulation of two or more spherical molecules,[1-3] nanoreactors,[4-5] or catalysts.[6-9] Carcerands and hemi-carcerands,[10-11] which are composed of covalently inked cavitands, are interesting types of single molecular capsules. In contrast to self-assembled capsules wherein the components are held together by noncovalent interactions such as hydrogen,[12-21] chalcogen,[22] halogen,[23] and coordination bonds such as palladium–nitrogen coordination bonds,[24-27] covalently linked molecular containers are thermally and chemically stable, though their production is synthetically more difficult.

Self-assembly has been proven to be a reasonable method for producing covalently linked molecular containers due to error correction favoring kinetic products to thermodynamically stable ones.[28-31] Shionoya et al. reported the template-assisted synthesis of a covalent organic capsule.[29] They utilized olefin metathesis to covalently link the eight components of a preorganized capsule. Warmuth et al. demonstrated a one-pot synthesis of an octahedral nanocontainer molecule by dynamic covalent bonding followed by reduction of the resulting imine bonds.[30] Pablo et al. reported the dimerization of a calix[4]pyrrole scaffold by cyclic diamines.[32] Although these examples nicely showed the preparation of covalently linked molecular architectures, those capable of contraction and expansion of their structures by external stimuli or species concomitant with the switching of molecular recognition capabilities remained less explored.[33-34]

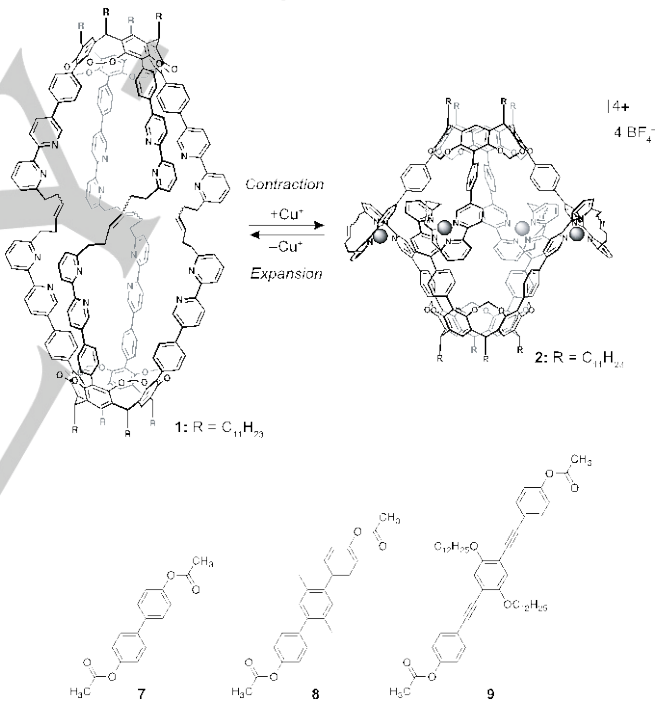

Figure 1. Schematic representation of interconverted between capsules **1** and **2** by metalation and demetalation. Guests **7**–**9**.

Recently, we demonstrated that substituents on the 6'-position of a 2,2'-bipyridyl arms on the wide-rim of resorcinarene-based capsules regulate the size of the inner cavity; [35] a *p*-methoxyphenyl-substituted capsule expanded the cavity by approximately 2 Å compared to its methyl-substituted counterpart. This expansion is caused by interactions between the electron-rich *p*-methoxyphenyl group and the electron-deficient bipyridyl arm distorting the coordination environments of the four metal centers. Although the degree of expansion was not very large, the *p*-methoxyphenyl-substituted capsule hosted a long alkyl chain that cannot be encapsulated by the methyl-substituted one.[36] These results indicate that the molecular

[a] K. Harada, Prof. Dr. R. Sekiya, Prof. Dr. T. Haino
Department of Chemistry, Graduate School of Science
Hiroshima University
1-3-1 Kagamiyama, Higashi-Hiroshima, Hiroshima, 739-8526 Japan
E-mail: haino@hiroshima-u.ac.jp

Supporting information for this article is given via a link at the end of the document.((Please delete this text if not appropriate))

recognition capability of the capsule can be reversibly switched when the cavity size is regulated by external species. These findings led us to design a new molecular capsule with a regulable internal cavity.

Herein, we report a resorcinarene-based hemicarcerand with a regulable internal cavity (**1**) (Figure 1). An olefin group was incorporated at the 6'-position of the bipyridyl arms. The formation of a carbon-carbon bond between the olefin groups by a second-generation Grubbs catalyst resulted in the title hemicarcerand. The covalently linked bipyridyl arms permitted the contraction and expansion of the internal cavity via metalation and demetallation, respectively, which can be applied to the switching of the molecular recognition capability.

Results and Discussion

Cavitand **4** was prepared by the procedure shown in Scheme S1 in the Supporting Information. Cavitand **4** was dimerized by mixing **4** and 2 equiv. of $[Cu(CH_3CN)_4](BF_4)$ in a mixed solvent solution of acetonitrile and dichloromethane (1:1, v/v) to produce capsule **3** as a reddish brown solid in quantitative yield. Metal-ligand coordination on **4** induced changes in the chemical shifts of the protons on the 2,2'-bipyridyl arms similar to those reported previously (Figure 2a and b).[36-39] The formation of **3** was confirmed by NOESY and ESI MS spectra.

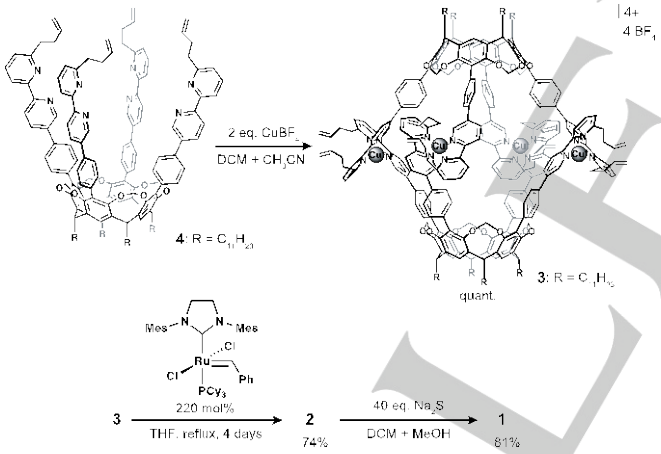

Scheme 1. Synthesis of capsule **1**.

Olefin metathesis on the vertexes of **3** was realized by a Grubbs second-generation catalyst. The reaction was found to be influenced by the solvents. In dichloromethane, the reaction gave complex mixtures, while the reaction in THF produced **2** as a main product. Previously, we reported that the rate of the helicity inversion of Cu-coordinated capsules in THF was much slower than that in dichloromethane.[36] Hence, the slow inversion of **3** in THF is likely to be indicative of olefin metathesis. In addition, preorganization is of vital importance for successful carbon-carbon bond formation; the olefin metathesis of **4** in THF under similar reaction conditions gave no desired product. Capsule **2** was purified by size exclusion chromatography on S-X1 BioBeads using chloroform as an eluent to give the product in 74% isolated yield.

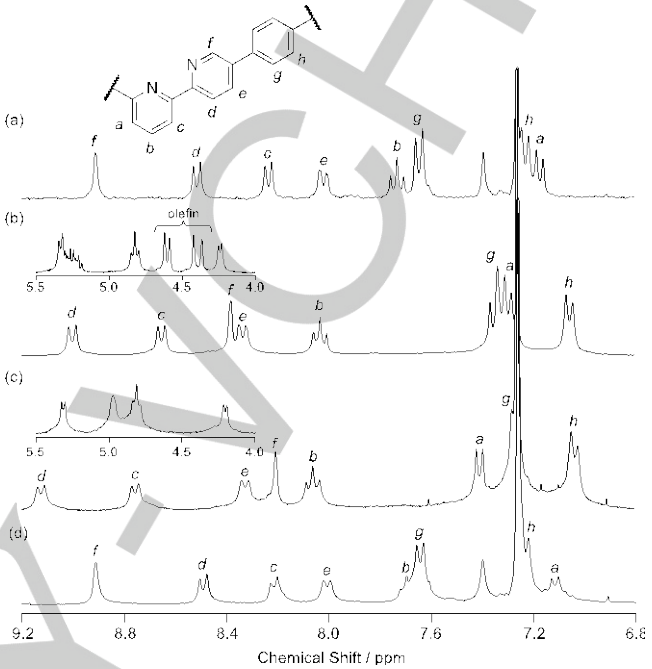

Figure 2. Selected region of ^{1}H NMR spectra (300 MHz, chloroform-d_1, 298 K) of (a) cavitand **4**, (b) capsule **3**, (c) capsule **2**, and (d) capsule **1**.

The carbon-carbon bond formation was confirmed by ^{1}H NMR spectroscopy. The signals corresponding to the terminal olefin moiety disappeared completely after the reaction (inset in Figure 2b and c). The ESI-MS spectrum verified the reaction completion. Ion peaks corresponding to $[\mathbf{2}]^{4+}$, $[\mathbf{2}+BF_4]^{3+}$, and $[\mathbf{2}+2BF_4]^{2+}$ were observed. The signals of the alkyl chain on the bipyridyl arms split into two signals because the folded conformation of the alkyl chains resulted in diastereotopic protons (Figure S19 in the Supporting Information).

The stereochemistry of the olefin moieties in **2** was estimated to be *trans*. Figure 3a illustrates model compounds of capsules **3** (model-**3**) and **2** (*trans*- and *cis*-model-**2**). The three model structures were optimized by the *Gaussian09* program at the M06-2X/6-31G(d,p)+LanL2DZ level of theory.[40] The dihedral angle between the two 2,2'-bipyridyl arms of model-**3** is 118.39°, which is larger than that of *trans*-model-**2**. The smaller dihedral angle of *trans*-model-**2** is caused by the covalent linkage between the bipyridyl arms. The dihedral angle of *cis*-model-**2** (45.24°) was estimated to be much smaller than those of the other structures. The distorted coordination environments reflected the stability; *cis*-model-**2** was calculated to be less stable by 15.71 kJ mol^{-1} than *trans*-model-**2**. Hence, capsule **2** with all *cis* forms is unlikely to be formed.

The UV-vis absorption spectra were consistent with the *trans* stereoisomer. The metal-to-ligand charge transfer (MLCT) band of the coordination capsules was found to be sensitive to

the coordination environment of the metal centers.[36, 41] For example, the MLCT band of the methyl-substituted capsule was observed at λ_{max} = 462 nm (green line in Figure 3b), while the *p*-methoxyphenyl-substituted one was shifted to λ_{max} = 547 nm (blue line in Figure 3b). The dihedral angles of the bipyridyl arms of the methyl- and *p*-methoxyphenyl-substituted capsules were determined by single-crystal X-ray diffraction studies to be 98.6° and 124.4°, respectively.[35-36] The UV-vis absorption spectra of **2** and **3** showed MLCT bands at λ_{max} = 450 nm for **2** and 456 nm for **3** (Figure 3b), both of which were similar to the MLCT band of the methyl-substituted capsule. Hence, the *trans* form was likely to be formed by olefin metathesis.

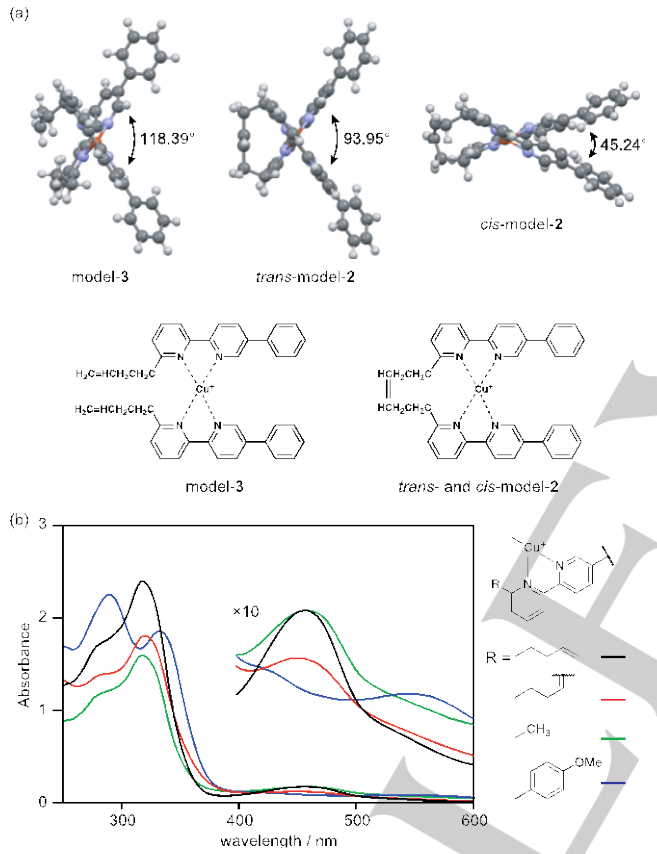

Figure 3. (a) Energy-minimized structures of three model compounds, model-**3**, *trans*-model-**2**, and *cis*-model-**2**. Color scheme: gray (carbon), white (hydrogen), light blue (nitrogen), red (oxygen). The model structures were calculated by the *Gaussian09* program at the M06-2X/6-31G(d,p)+LanL2DZ level of theory. (b) UV-vis absorption spectra (THF, 298 K) of **2** (red), **3** (black), *p*-methyl-substituted capsule (green), and *p*-methoxyphenyl-substituted capsule (blue). The concentrations of the capsules are 1.0×10^{-2} mM.

Demetalation was accomplished by the reaction of **2** with 40 equiv. of sodium sulfide in a mixed solvent solution of methanol and dichloromethane (1:1, v/v) at room temperature. Filtration followed by GPC purification gave **1** in 81% isolated yield. Demetalation was confirmed by ^{1}H NMR spectroscopy; the chemical shifts of the 2,2'-bipyridyl arms of **1** were similar to those of **4**. The removal of the Cu^+ ions was confirmed by NOESY and ESI-MS spectra. The NOESY spectrum showed the disappearance of NOEs between the aliphatic chain and bipyridyl arm, which was observed in **2**. ESI-MS showed molecular ion peaks corresponding to $[\mathbf{1}+4H]^{4+}$, $[\mathbf{1}+3H]^{3+}$, and $[\mathbf{1}+2H]^{2+}$, while no ion peaks attributed to Cu^+–containing capsules were detected.

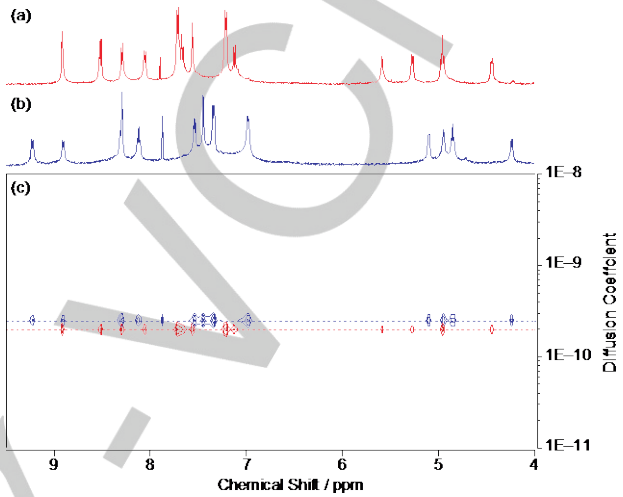

Figure 4. Selected region of ^{1}H NMR spectra (500 MHz, 298 K, THF-d_8) of (a) **1** and (b) **2**. (c) ^{1}H DOSY spectra (500 MHz, 298 K, THF-d_8) of **1** and **2**. The ^{1}H DOSY spectrum of **2** is superimposed over that of **1**.

^{1}H DOSY determined that the diffusion constant of **2** was $3.47(2) \times 10^{-10}$ m^2 s^{-1}, which was larger than the value of $3.01(4) \times 10^{-10}$ m^2 s^{-1} for **1** (Figure 4). The hydrodynamic radii were calculated by the Stocks-Einstein equation to be 13.3(1) Å for **2** and 15.3(2) Å for **1**. These results suggested an approximately 4 Å expansion of **1**. The expanded structure can be reproduced by molecular mechanics calculations by MacroModel Ver. 9.0 program using the MMFFs force[42] field (Figure. S35 in Supporting Information). The heights of **1** and **2**, which were defined as the distances between the centroids of the four carbon atoms at the wide rim of the resorcinarene cavitand, were estimated to be 19.7 and 15.9 Å, respectively. The 3.8 Å expansion was in good agreement with that estimated by the DOSY measurements.

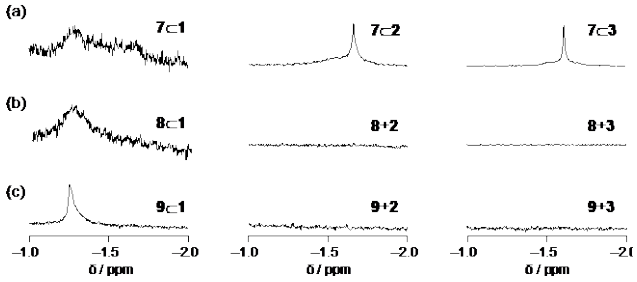

Figure 5. Selected region of the ^{1}H NMR spectra (500 MHz, 223 K, chloroform-d_1) of (a) mixtures of capsule (**1**, **2**, or **3**) and **7**, (b) mixtures of

capsule (**1**, **2**, or **3**) and **8**, and (c) mixtures of capsule (**1**, **2**, or **3**) and **9**. The concentration of the capsules was 0.2 mM.

To gain insight into the molecular recognition capabilities of the capsules, host-guest complexation experiments were carried out. Three guests, 4,4'-diacetoxybiphenyl **7**, 1,4-bis(4-acetoxyphenyl)-2,5-dimethyl benzene **8**, and 1,4-bis(4-acetoxyphenylethyny)-2,5-di(dodecanyloxy)benzene **9**, were employed. Long alkyl chains were incorporated into **9** to improve the solubility in organic solvents. Molecular mechanics calculations estimated the distance between the ester oxygen atoms to be 9.876, 14.155, and 19.267 Å, respectively (Figure. S36 in the Supporting Information).[43]

The chemical shift of the acetoxy group of the linear guests reflects the size of the capsule; as the height of the capsule increases, the bound guest experiences a lower shielding effect from the surrounding aromatic rings of the resorcinarene scaffold, responding to the down-field shift of the signal. At room temperature, the acetoxy group of **7** bound in **2** and **3** gave rise to resonances in the high-field region, indicative of the formation of the host-guest complexes **7**⊂**3** and **7**⊂**2**, while no signal corresponding to the bound guest was detected in **1** due to rapid exchange between the bound and unbound guests. At –50 °C, the ^{1}H NMR spectra of **2** and **3** displayed signals attributed to the bound guests at δ = –1.67 and –1.61 ppm, respectively, while a broad signal with a peak at δ = –1.29 ppm was found in the case of **1** (Figure. 5a). The observed chemical shift indicated that **2** has the smallest inner cavity and that **1** has the largest inner cavity. Association constants (K_a) at room temperature demonstrated that capsule **1** weakly recognized **7** as expected by its larger inner cavity (Table 1).[44] The K_a value of **2** was found to be smaller than that of **3**.

Table 1. Association constants (Ka / L mol^{-1}) of **7**–**9** in capsules **1**–**3** at 298 K.[a]

	Ka / L mol^{-1}		
	Guest **7**	Guest **8**	Guest **9**
Capsule **1**	7.6(3)	12(1)	3.6(2) × 10^2
Capsule **2**	1.8(3) × 10^4	N.B.	N.B.
Capsule **3**	4.0(2) × 10^4	N.B.	N.B.

[a] Association constants were determined by the ^{1}H NMR spectra using a 1:1 host-to-guest binding model. N.B. = not bound.

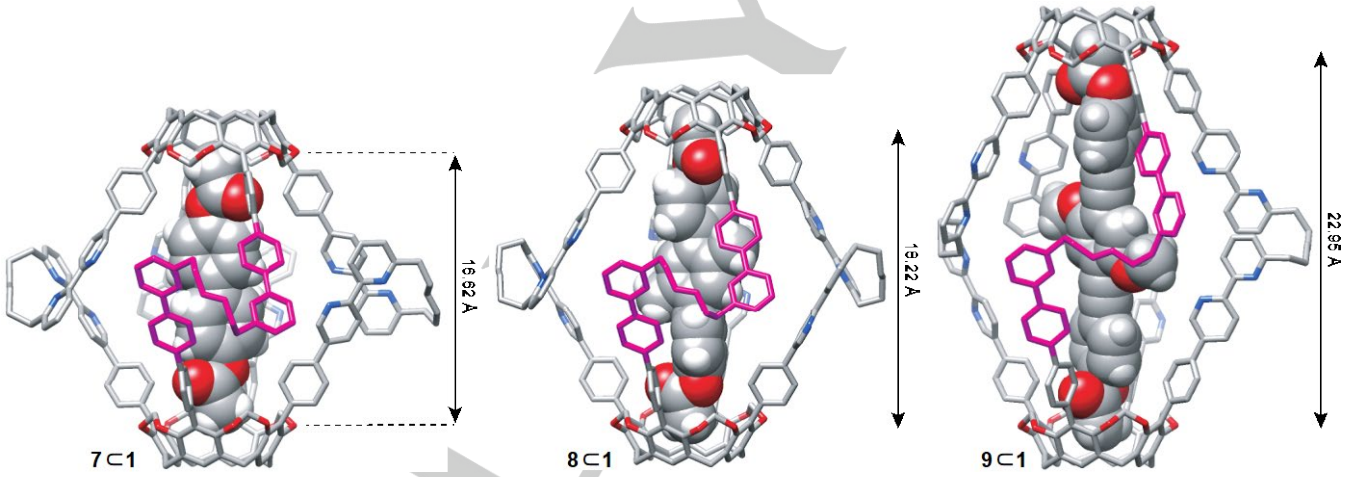

Figure 6. Energy-minimized structures of the host-guest complexes, **7**⊂**1**, **8**⊂**1**, and **9**⊂**1**. The MMFF force field was employed for the geometry optimizations. The hydrogen atoms of **1** are omitted for clarity. The height of the capsule is defined by the distance between the centroids of the four carbon atoms at the wide rim of the resorcinarene cavitand. Color scheme: gray (carbon), white (hydrogen), blue (nitrogen), red (oxygen).

Guest **8** was captured only by **1** (Figure 5b). Again, a broad signal was found in the high-field region at –50°C. The expanded structure of **1** was demonstrated by the encapsulation of **9** (Figure 5c). Interestingly, the acetoxy groups of **7**–**9** bound in **1** resulted in resonances at a similar chemical shift, albeit the fact that the three guests have different lengths. This indicates that the distances between the resorcinarene cavitand and the methyl groups at the termini of the guests were similar in all host-guest complexes. Most likely, the conformationally flexible covalent linkages regulated the inner cavity to realize similar environments. Capsule **1** recognized **8** with an affinity similar to that for **7**, while the K_a value increased to 3.6(2) × 10^2 M^{-1} in the case of **9**, indicating that capsule **1** prefers the long guest.

Figure 6 displays energy-minimized structures of the host-guest complexes, **7**⊂**1**, **8**⊂**1**, and **9**⊂**1**. The structures were optimized by the MacroModel ver.9.0 program using the MMFF force field. The calculations demonstrated that capsule **1** regulates its inner cavity by changing the conformation of the bipyridyl arms. When the shortest guest is hosted by **1**, the bipyridyl arms, which are shown in purple, adopted folded conformations. As the length of the bound guests increased, the folded conformations gradually unfolded to adapt the inner cavity

to the guests. These changes increase the height of **1** from 16.62 Å to 22.95 Å. This conformational change explained why the binding constant of **9** was the highest among the three guests. The molecular mechanics calculation predicted a maximum height of approximately 28 Å when the alkyl chains adopted extended conformations (Figure S37 in Supporting Information), demonstrating the highly flexible and regulable structure of **1**.

The bipyridyl arms can coordinate with the Cu^+ ions, inducing capsule **1** to form a compressed structure. This metal-induced structural change can be used to regulate guest preference. In chloroform-d_1, wherein equimolar amounts of **7**–**9** coexisted, capsule **1** selectively captured **9** (Figure. 7a), while the addition of $[Cu(NCCH_3)_4](BF_4)$ to the solution shifted the guest preference from **9** to **7** due to the contraction of the cavity by the regulation of **2** (Figure 7b). The preferred guest can be restored by the addition of 32 equiv. of ethylenediamine into the solution (Figure 7c). The elimination of the Cu^+ cations enabled the capsule to expand its inner cavity, and **9** was again hosted by the resulting capsule **1**.

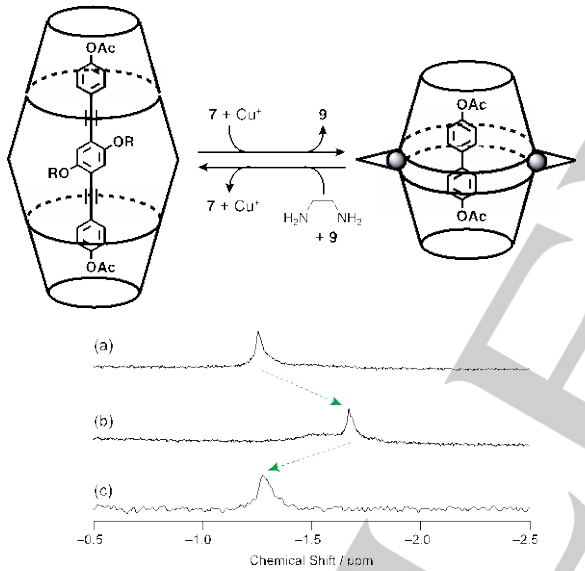

Figure 7. Selected region of the ^{1}H NMR spectra (500 MHz, chloroform-d_1, 223 K) of (a) a mixture of guests **7**–**9** (4.0 mM each) and capsule **1** (0.2 mM), (b) after addition of 4 equiv. of $[Cu(CH_3CN)_4]BF_4$ into the mixture, and (c) after the addition of 32 equiv. ethylenediamine into the solution.

Conclusions

In conclusion, a resorcinarene-based hemi-carcerand was realized by metal-directed dimerization followed by olefin metathesis at the vertexes of the resulting metal-coordinated capsule with a second-generation Grubbs catalyst. This procedure enabled the production of a covalently linked container molecule in a good isolated yield. The ^{1}H DOSY measurements and the molecular mechanics calculations demonstrated the highly flexible and regulable structure of the molecular capsule resulting from carbon-carbon bond formation between the two 2,2'-bipyridyl arms. The regulable structure enabled encapsulation from 4,4'-diacetoxybiphenyl to 2,5-disubstituted-1,4-bis(4-acetoxyphenylethynyl)benzene, which is longer by 9.4 Å than the former. The Lewis base bipyridyl moieties embedded in the bipyridyl arms permitted the contraction and expansion of the capsule via metalation and demetalation of Cu^+, enabling regulation of the molecular recognition capability. This stimuli-responsible structural change is applicable to the development of functional supramolecular systems that can control the uptake, transfer and release of chemicals. Accordingly, we are now developing multi-component systems utilizing the molecular recognition capability of the hemi-carcerand.

Experimental Section

General

All chemicals and solvents were purchased from Kanto Chemical Co., Ltd., Wako Pure Chemical Co., Ltd., Tokyo Kasei Kogyo Co., Ltd., and Sigma-Aldrich Co., Ltd., and were used as received without further purification. ^{1}H and ^{13}C NMR spectra were recorded on VARIAN 300 MHz, JEOL ECA-500 MHz and ECA-600 MHz spectrometers. ^{1}H DOSY spectra were recorded on a JEOL ECA-500 MHz spectrometer. Chemical shifts are quoted as parts per million (ppm) relative to chloroform (chloroform-d_1, δ = 7.26 ppm for ^{1}H and 77.2 ppm for ^{13}C) or tetrahydrofuran (tetrahydrofuran-d_8, δ = 3.58 ppm for 1H). IR spectra were recorded on a JASCO FT/IR-4600 spectrometer with an attenuated total reflectance apparatus. UV/vis absorption spectra were recorded on a JASCO V-560 spectrophotometer. High-resolution mass spectra (HRMS) were recorded on a Thermo Fisher Scientific LTQ Orbitrap XL by electron splay ionization (ESI) method. Melting points were measured with a Yanagimoto micro melting point apparatus and uncorrected. The synthesis of the 2,2'-bipyridyl arm and the guests were compiled in the Supporting Information.

Computational Methods

The geometry optimizations of model compounds, model-**3** and *trans*- and *cis*-model-**2**, were carried out by the *Gaussian 09* program using M06-2X/6-31G(d,p)+LanL2DZ level of theory. The 6-31G(d,p) basis set was applied for the carbon, hydrogen, and nitrogen atoms. The LanL2DZ basis set was applied for the cupper ion. The cartesian coordinates of the optimized structures are listed in Tables S1–S3.

The energy minimizations of **1**, **2**, **7**⊂**1**, **8**⊂**1**, and **9**⊂**1** were carried out by the *MacroMode*l Ver. 9.0 program using MMFFs force field. The molecular structures of **1** and **2** were shown in Figures S35 and S37. The stereochemistry of the olefin moieties of **1** and **2** was fixed to be *trans*. The Cu^+ cations were replaced with the carbon atoms and the long alkyl chains were replaced with the hydrogen atoms. The bond distance between the nitrogen and the carbon atoms were fixed to be 2.0 Å due to the fact that the X-ray crystal structure of a methyl-substituted capsule revealed the bond distance between the cupper and the nitrogen atoms of 2.0 Å in average. The DFT calculation of *trans*-model-**2** suggested that dihedral angle between the bipyridyl groups was 93.95°. Hence, the dihedral angles between the bipyridyl arms were fixed to be 93.95°.

The energy minimization of **7**–**9** were carried out by the *MacroModel* Ver. 9.0 program using MMFFs force field. The dodecyl

chains of **9** were replaced with the methyl groups. The molecular structures of **7**–**9** were shown in Figure S36 in the Supporting Information.

Synthesis of 4

A mixture of 6'-(3''-butenyl)-5-(4-(4,4,5,5-tetramethyl-1,3,2-dioxaborolan-2-yl)phen-yl)-2,2'-bipyridine (**6**) (559 mg, 1.35 mmol), triphenylarsine (138 mg, 0.451 mmol), tetraiodocavitand (188 mg, 0.113 mmol), dichlorobis(triphenylphosphine)palladium (15.8 mg, 22.5 μmol. 20 mol%), and cesium carbonate (1.12 g, 3.44 mmol) was dissolved in a mixed solvent solution of dioxane (10.6 mL) and water (0.42 mL). After stirring for 3 hours at 110 °C in the dark, the reaction mixture was cooled to room temperature and was filtered through celite. The solution was concentrated under reduced pressure. The organic residue was purified by GPC (chloroform) to afford cavitand **4** as yellow solid in 80% yield (207 mg, 90.4 μmol).

M.p.: >300 °C ; ^{1}H NMR (300 MHz, chloroform-d_1): δ 8.91 (d, 4H, J = 1.9 Hz), 8.51 (d, 4H, J = 8.2 Hz), 8.23 (d, 4H, J = 7.7 Hz), 8.02 (dd, 4H, J = 8.2, 1.9 Hz), 7.73 (t, 4H, J = 7.7 Hz), 7.64 (d, 8H, J = 8.2 Hz), 7.39 (s, 4H), 7.23 (d, 8H, J = 8.2 Hz), 7.17 (d, 4H, J = 7.7 Hz), 5.93 (m, 4H), 5.43 (d, 4H, J = 6.9 Hz), 5.08 (dd, 4H, J = 17.2, 1.8 Hz), 4.99 (dd, 4H, J = 10.2, 1.8 Hz), 4.92 (t, 4H, J = 8.1 Hz), 4.40 (d, 4H, J = 6.9 Hz), 2.98 (t, 8H, J = 7.1 Hz), 2.59 (m, 8H), 2.46 - 2.31, 1.75 -1.22 (br, 80H), 0.90 (t, 12H, J = 6.7 Hz) ppm; ^{13}C NMR (75 MHz, chloroform-d_1): δ 161.0, 155.6, 155.3, 152.8, 147.6, 138.6, 138.1, 137.2, 136.6, 135.7, 135.1, 134.0, 130.9, 128.8, 126.7, 123.0, 121.2, 120.3, 118.5, 115.1, 100.8, 37.7, 37.3, 33.7, 32.1, 30.7, 30.1, 29.9, 29.6, 28.2, 25.1, 22.9, 14.4 ppm; IR (ATR): ν 2922, 2851, 1590, 1571, 1425, 1396, 1361, 1308, 1251, 1155, 1084, 1018, 911, 859, 832 cm^{-1}; HRMS(ESI+) calcd for $C_{156}H_{178}O_8N_8$, m/z 1145.68783 $[M+2H]^+$, found m/z 1145.69090.

Synthesis of 3

A solution of **4** (207 mg, 90.4 μmol) and tetrakis(acetonitrile)cupper tetrafluoroborate (53.9 mg, 0.171 mmol) in a mixed solvent solution of acetonitrile (5 mL) and dichloromethane (5 mL) was stirred at room temperature for 30 min to afford **3**$(BF_4)_4$ as reddish brown solid in quantitative yield.

M.p.: >300 °C ; ^{1}H NMR (300 MHz, chloroform-d_1): δ 9.01 (d, 8H, J = 8.1 Hz), 8.65 (d, 8H, J = 7.9 Hz), 8.38 (s, 8H), 8.34 (d, 8H, J = 8.1 Hz), 8.03 (t, 8H, J = 7.9 Hz), 7.47–7.22 (m, 32H), 7.05 (d, 16H, J = 7.9 Hz), 5.40-5.16 (m, 16H), 4.82 (t, 8H, J = 7.7 Hz), 4.60 (d, 8H, J = 10.1 Hz), 4.39 (d, 8H, J = 16.7 Hz), 4.24 (d, 8H, J = 6.7 Hz), 2.64 (t, 16 H, J = 7.4 Hz), 2.40-1.92, 1.62-1.11 (m, 176 H), 0.88 (t, 24H, J = 6.7 Hz) ppm; ^{13}C NMR (150 MHz, chloroform-d_1): δ 159.7, 152.7, 152.3, 152.2, 151.1, 146.6, 139.3, 138.8, 138.7, 138.6, 137.3, 136.1, 135.8, 133.6, 131.2, 128.0, 126.9, 124.9, 124.3, 120.9, 120.2, 115.5, 100.8, 39.3, 37.2, 33.4, 32.1, 30.6, 29.9, 29.9, 29.5, 28.0, 24.9, 22.8, 14.3 ppm; IR (ATR): ν 2922, 2851, 1596, 1567, 1452, 1397, 1362, 1306, 1252, 1157, 1057, 1017, 962, 831, 807 cm^{-1}; HRMS(ESI+) calcd for $C_{312}H_{352}O_{16}N_{16}BCu_4F_4$ $[M+BF_4]^{3+}$, m/z 1639.14444, found m/z 1639.14730.

Synthesis of 2

To a solution of **3** (20 mg, 3.9 μmol) in dry tetrahydrofuran (20 mL), Grubbs second catalyst (1.8 mg, 2.1 μmol) was added. The solution was refluxed for 24 hours under N_2 atmosphere. Grubbs second catalyst (1.8 mg, 2.1 μmol) and dry tetrahydrofuran (2 mL) was added to the solution. The solution was refluxed for 24 hours. This process was repeated by three times. The solvent was removed under reduced pressure. The residual solid was purified by BioBeads S-X1 (chloroform) to give capsule **2**$(BF_4)_4$ as reddish brown solid in 74% isolated yield (14.8 mg, 2.92 μmol).

M.p.: >300 °C ; ^{1}H NMR (600 MHz, chloroform-d_1): δ 9.10 (d, 8H, J = 8.2 Hz), 8.75 (d, 8H, J = 7.8 Hz), 8.32 (dd, 8H, J = 8.2, 1.9 Hz), 8.21 (d, 8H, J = 1.9 Hz), 8.06 (t, 8H, J = 7.8 Hz), 7.41 (d, 8H, J = 7.8 Hz), 7.30-7.25 (br, 24H), 7.04 (d, 16H, J = 7.0 Hz), 5.32 (d, 8H, J = 6.7 Hz), 5.01-4.94 (br, 8H), 4.82 (t, 8H, J = 7.8 Hz), 4.21 (d, 8H, J = 6.7 Hz), 3.03-2.91 (br, 8H), 2.68-2.55 (br, 8H), 2.15-2.04 (br, 8H), 2.43-2.17, 1.67-1.02, 0.98-0.75 (br, 192H) ppm; ^{13}C NMR (150 MHz, chloroform-d_1): δ 159.8, 152.7, 152.3, 151.5, 151.3, 146.2, 139.4, 138.7, 138.5, 137.6, 136.1, 133.3, 131.2, 130.5, 127.9, 127.1, 125.3, 124.2, 120.9, 120.2, 100.8, 42.4, 37.2, 32.1, 30.6, 29.9, 29.9, 29.8, 29.5, 28.0, 22.8, 14.2 ppm; IR (KBr): ν 2924, 2852, 1754, 1598, 1568, 1456, 1397, 1364, 1261, 1159, 1084, 1020, 967, 807 cm^{-1}; HRMS(ESI+) calcd for $C_{304}H_{336}O_{16}N_{16}BCu_4F_4$ $[M+BF_4]^{3+}$, m/z 1601.77224, found m/z 1601.77530.

Synthesis of 1

To a solution of **2** (195 mg, 38.5 μmol) in dichloromethane (15 mL) was added a solution of sodium sulfide (375 mg, 1.56 mmol) in MeOH (15 mL). The solution was stirred at room temperature for 30 min. The solvent was removed under reduced pressure. The residue was extracted with chloroform and ammonium chloride. The organic layer was dried over anhydrous sodium sulfate and evaporated. The product was purified by column chromatography on BioBeads S-X1 (eluent = THF) to give carbon capsule **1** in 81% (140 mg, 31.3 μmol).

M.p.: >300 °C ; ^{1}H NMR (500 MHz, chloroform-d_1): δ 8.91 (s, 8H), 8.48 (d, 8H, J = 8.1 Hz), 8.21 (d, 8H, J = 7.7 Hz), 8.00 (dd, 8H, J = 8.1, 2.0 Hz), 7.69 (t, 8H, J = 7.7 Hz), 7.64 (d, 16H, J = 7.9 Hz), 7.40 (s, 8 H), 7.23 (d, 16 H, J = 7.9 Hz), 7.11 (d, 8H, J = 7.7 Hz), 5.61-5.55 (br, 8H), 5.43 (d, 8H, 6.1 Hz), 4.94 (t, 8H, J = 7.3 Hz), 4.40 (d, 8H, J = 6.1 Hz), 2.90 (t, 16H, J = 7.2 Hz), 2.56-2.45 (br, 16H), 2.45-2.30, 1.62-1.13, 0.96-0.78 (br, 184H) ppm; ^{13}C NMR (125 MHz, chloroform-d_1): δ 161.3, 155.7, 155.3, 152.9, 147.7, 138.6, 137.1, 136.6, 135.7, 135.0, 134.0, 130.9, 130.3, 128.8, 126.7, 121.2, 118.5, 100.9, 38.5, 37.3, 32.6, 32.1, 30.7, 30.0, 29.9, 29.6. 28.2, 22.9, 14.3 ppm; IR (ATR): ν 2922, 2851, 1570, 1450, 1256, 1155, 1083, 962, 804 cm^{-1}; HRMS(ESI+) calcd for $C_{304}H_{339}O_{16}N_{16}$ $[M+3H]^{3+}$, m/z 1489.87295, found m/z 1489.87451.

Author Contributions

†These authors contributed equally to this work.

Acknowledgements

This work was supported by JSPS KAKENHI Grant Numbers 18K05085, JP17H05375, JP19H04585, and JP17H05159. Funding from The Ogasawara Foundation for the Promotion of Science & Engineering, The Futaba Electronics Memorial Foundation, Nippon Sheet Glass Foundation, Iketani Science and Technology Foundation, Takahashi Industrial and Economic Research Foundation, and Fukuoka Naohiko Memorial Foundation are gratefully acknowledged.

Keywords: host-guest chemistry • supramolecular chemistry • carcerand • resorcinarene • molecular recognition

[1] K. Mahata, P. D. Frischmann, F. Wurthner, *J. Am. Chem. Soc.* **2013**, *135*, 15656-15661.
[2] F. J. Rizzuto, D. M. Wood, T. K. Ronson, J. R. Nitschke, *J. Am. Chem. Soc.* **2017**, *139*, 11008-11011.
[3] K. Matsumoto, S. Kusaba, Y. Tanaka, Y. Sei, M. Akita, K. Aritani, M. Haga, M. Yoshizawa, *Angew. Chem. Int. Ed.* **2019**, *58*, 8463-8467.
[4] J. Chen, J. Rebek Jr., *Org. Lett.* **2002**, *4*, 327-329.
[5] J. M. Kang, J. Rebek, *Nature* **1997**, *385*, 50-52.
[6] Z. Lu, R. Lavendomme, O. Burghaus, J. R. Nitschke, *Angew. Chem. Int. Ed.* **2019**, *58*, 9073-9077.
[7] M. Yoshizawa, M. Tamura, M. Fujita, *Science* **2006**, *312*, 251-254.
[8] W. M. Hart-Cooper, K. N. Clary, F. D. Toste, R. G. Bergman, K. N. Raymond, *J. Am. Chem. Soc.* **2012**, *134*, 17873-17876.
[9] D. Fiedler, H. van Halbeek, R. G. Bergman, K. N. Raymond, *J. Am. Chem. Soc.* **2006**, *128*, 10240-10252.
[10] A. Jasat, J. C. Sherman, *Chem. Rev.* **1999**, *99*, 931-967.
[11] D. J. Cram, S. Karbach, Y. H. Kim, L. Baczynskyj, G. W. Kalleymeyn, *J. Am. Chem. Soc.* **1985**, *107*, 2575-2576.
[12] K. D. Shimizu, J. Rebek Jr., *Proc. Natl. Acad .Sci. USA* **1995**, *92*, 12403-12407.
[13] R. K. Castellano, D. M. Rudkevich, J. Rebek Jr., *J. Am. Chem. Soc.* **1996**, *118*, 10002-10003.
[14] P. Ballester, G. Gil-Ramírez, *Proc. Natl. Acad .Sci. USA* **2009**, *106*, 10455-10459.
[15] A. Díaz-Moscoso, F. A. Arroyave, P. Ballester, *Chem. Commun.* **2016**, *52*, 3046-3049.
[16] L. Osorio-Planes, M. Espelt, M. A. Pericàs, P. Ballester, *Chem. Sci.* **2014**, *5*, 4260-4264.
[17] R. Sekiya, A. Díaz-Moscoso, P. Ballester, *Chem.-Eur. J.* **2018**, *24*, 2182-2191.
[18] D. Ajami, J. Rebek Jr., *J. Am. Chem. Soc.* **2006**, *128*, 15038-15039.
[19] D. Ajami, J. Rebek Jr., *J. Am. Chem. Soc.* **2006**, *128*, 5314-5315.
[20] J. M. Kang, J. Rebek Jr., *Nature* **1997**, *385*, 50-52.
[21] R. K. Castellano, B. H. Kim, J. Rebek Jr., *J. Am. Chem. Soc.* **1997**, *119*, 12671-12672.
[22] L. J. Riwar, N. Trapp, K. Root, R. Zenohi, F. Diederich, *Angew. Chem. Int. Ed.* **2018**, *57*, 17259-17264.
[23] N. K. Beyeh, F. Pan, K. Rissanen, *Angew. Chem. Int. Ed.* **2015**, *54*, 7303-7307.
[24] L. Escobar, E. C. Escudero-Adan, P. Ballester, *Angew. Chem. Int. Ed.* **2019**, 10.1002/anie.201909685.
[25] M. Yamanaka, Y. Yamada, Y. Sei, K. Yamaguchi, K. Kobayashi, *J. Am. Chem. Soc.* **2006**, *128*, 1531-1539.
[26] K. Kobayashi, Y. Yamada, M. Yamanaka, Y. Sei, K. Yamaguchi, *J. Am. Chem. Soc.* **2004**, *126*, 13896-13897.
[27] F. Fochi, P. Jacopozzi, E. Wegelius, K. Rissanen, P. Cozzini, E. Marastoni, E. Fisicaro, P. Manini, R. Fokkens, E. Dalcanale, *J. Am. Chem. Soc.* **2001**, *123*, 7539-7552.
[28] N. Nishimura, K. Kobayashi, *Angew. Chem. Int. Ed.* **2008**, *47*, 6255-6258.
[29] S. Hiraoka, Y. Yamauchi, R. Arakane, M. Shionoya, *J. Am. Chem. Soc.* **2009**, *131*, 11646-11647.
[30] X. J. Liu, Y. Liu, G. Li, R. Warmuth, *Angew. Chem. Int. Ed.* **2006**, *45*, 901-904.
[31] K. Tamaki, A. Ishigami, Y. Tanaka, M. Yamanaka, K. Kobayashi, *Chem.-Eur. J.* **2015**, *21*, 13714-13722.
[32] A. Galan, E. C. Escudero-Adan, P. Ballester, *Chem. Sci.* **2017**, *8*, 7746-7750.
[33] R.-J. Li, J. J. Holstein, W. G. Hiller, J. Andréasson, G. H. Clever, *J. Am. Chem. Soc.* **2019**, *141*, 2097-2103.
[34] R.-J. Li, M. Han, J. Tessarolo, J. J. Holstein, J. Lübben, B. Dittrich, C. Volkmann, M. Finze, C. Jenne, G. H. Clever, *ChemPhotoChem* **2019**, *3*, 378-383.
[35] T. Maehara, R. Sekiya, K. Harada, T. Haino, *Org. Chem. Front.* **2019**, *6*, 1561-1566.
[36] T. Imamura, T. Maehara, R. Sekiya, T. Haino, *Chem.-Eur. J.* **2016**, *22*, 3250-3254.
[37] Y. Tsunoda, K. Fukuta, T. Imamura, R. Sekiya, T. Furuyama, N. Kobayashi, T. Haino, *Angew. Chem. Int. Ed.* **2014**, *53*, 7243-7247.
[38] T. Haino, M. Kobayashi, Y. Fukazawa, *Chem.-Eur. J.* **2006**, *12*, 3310-3319.
[39] T. Haino, M. Kobayashi, M. Chikaraishi, Y. Fukazawa, *Chem. Commun.* **2005**, 10.1039/b502598b, 2321-2323.
[40] *Gaussian 09*, Revision D.01. M. J. Frisch, G. W. Trucks, H. B. Schlegel, G. E. Scuseria, M. A. Robb, J. R. Cheeseman, G. Scalmani, V. Barone, B. Mennucci, G. A. Petersson, H. Nakatsuji, M. Caricato, X. Li, H. P. Hratchian, A. F. Izmaylov, J. Bloino, G. Zheng, J. L. Sonnenberg, M. Hada, M. Ehara, K. Toyota, R. Fukuda, J. Hasegawa, M. Ishida, T. Nakajima, Y. Honda, O. Kitao, H. Nakai, T. Vreven, J. J. A. Montgomery, J. E. Peralta, F. Ogliaro, M. Bearpark, J. J. Heyd, E. Brothers, K. N. Kudin, V. N. Staroverov, R. Kobayashi, J. Normand, K. Raghavachari, A. Rendell, J. C. Burant, S. S. Iyengar, J. Tomasi, M. Cossi, N. Rega, J. M. Millam, M. Klene, J. E. Knox, J. B. Cross, V. Bakken, C. Adamo, J. Jaramillo, R. Gomperts, R. E. Stratmann, O. Yazyev, A. J. Austin, R. Cammi, C. Pomelli, J. W. Ochterski, R. L. Martin, K. Morokuma, V. G. Zakrzewski, G. A. Voth, P. Salvador, J. J. Dannenberg, S. Dapprich, A. D. Daniels, Ö. Farkas, J. B. Foresman, J. V. Ortiz, J. Cioslowski, D. J. Fox, **2009**.
[41] K. Harada, R. Sekiya, T. Maehara, T. Haino, *Org. Biomol. Chem.* **2019**, *17*, 4729-4735.
[42] F. Mohamadi, N. G. J. Richards, W. C. Guida, R. Liskamp, M. Lipton, C. Caufield, G. Chang, T. Hendrickson, W. C. Still, *J. Comput. Chem.* **1990**, *11*, 440-467.
[43] The distance between the terminal methyl groups is 14.22 Å for **7**, 18.47 Å for **8**, and 23.51 Å for **9**.
[44] The association constant of **7**⊂**1** was determined by ^{1}H NMR titration experiment.

Entry for the Table of Contents (Please choose one layout)

Layout 1:

FULL PAPER

A Resorcinarene-based capsule with a regulable internal cavity was realized. The alkyl chains connecting 2,2;-bipyridyl arms permit to expand and contract the cavity by demetalation and metalation. A reversible size change of the capsule enable to switch its molecular recognition properties.

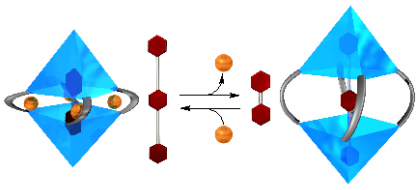

Kentaro Harada, Ryo Sekiya, and Takeharu Haino

Page No. – Page No.

A Regulable Internal Cavity Inside A Resorcinarene-Based Hemi-Carcerand